Measured Performance of a Multimegawatt MPD Thruster

R.L. Burton,* K.E. Clark,† and R.G. Jahn‡
Princeton University, Princeton, New Jersey

Thrust and efficiency of a quasisteady multimegawatt MPD thruster are determined by measuring the impulse bit per pulse on a swinging gate thrust stand in a dielectric vacuum tank at a background pressure of 10^{-4} Torr. The quasisteady thrust data scale quadratically with arc current and confirm previous estimates of the electromagnetic and electrothermal components of thrust from magnetic and pressure probe measurements. Thruster efficiency is found to increase monotonically with specific impulse, reaching a value of 28% at 2000 s for argon and 38% at 4000 s for nitrogen.

Nomenclature

B	= magnetic field
b	= constant defined by Eq. (7)
b_{em}	= constant defined by Eq. (1)
C	= constant in electromagnetic thrust equation
g	= gravitational acceleration
I	= thruster polar moment of inertia
I_{sp}	= specific impulse
J	= current
j	= current density
L	= inductance
$\dot{m}$	= mass flow rate
R	= radial distance from center of thrust to thrust stand rotational axis
r	= effective radius of current attachment
T	= thrust
t	= time
V	= voltage
x	= transducer measured thruster position
η	= thrust efficiency
μ_o	= permeability of free space
ω	= thrust stand angular velocity

Superscript

$( )^*$	= erosion onset condition

Subscripts

a	= anode
c	= cathode
em	= electromagnetic
et	= electrothermal

Introduction

THE magnetoplasmadynamic (MPD) thruster is an inherently simple device, consisting of a cylindrical cathode, an annular anode, chamber backplate and sidewall insulators, and propellant injectors. An axially symmetric arc current pattern produces an azimuthal magnetic field which reacts on the current to produce axial and radial body forces throughout the conducting plasma. Gasdynamic pressure forces generated as the propellant is heated by the discharge also contribute to the thrust.

The electromagnetic component, the dominant of the two thrust mechanisms, can be shown to vary quadratically with arc current, either by integration of the $j \times B$ body force over the volume of the arc chamber, or more generally by evaluation of the Maxwell stress tensor over a volume enclosing the arc current.[1] More specifically, this electromagnetic component is given by

$$T_{em} = (\mu_0/4\pi)\, J^2 [\ln(r_a/r_c) + C] \equiv b_{em} J^2 \tag{1}$$

where C is a constant of order 0.1 which depends on the distribution of current on the cathode tip.

The electrothermal component depends on propellant type, mass flow, and current and, for argon, can be described by the empirical relation[2]

$$T_{et} = 0.098\, (\dot{m})^{0.3}\, J^{1.5} \tag{2}$$

where $\dot{m}$ is in grams per second and J is in kiloamperes.

Since the electrothermal contribution is typically less than 10% of the total thrust, the specific impulse of the MPD thruster can be well approximated by

$$I_{sp} = T/\dot{m}g \approx b_{em} J^2/\dot{m}g \tag{3}$$

which would seem to imply that an arbitrarily high specific impulse can be attained as the ratio $J^2/\dot{m}$ is increased. In practice, however, there is an empirical limit to this ratio, termed the "onset" condition, $(J^2/\dot{m})^*$, above which arc operation is accompanied by high amplitude terminal voltage fluctuations and the erosion of the electrodes and insulators.[3-5] This onset parameter has been shown to be dependent on electrode size and shape, propellant type, and mass flow distribution, and efforts continue to be made to optimize these features.[6,7]

From these studies, new MPD configurations have evolved which show the promise of specific impulse and efficiency combinations of interest for a variety of advanced space missions. Unfortunately, while the understanding of the physics of MPD acceleration has improved substantially, until recently facilities at this laboratory have not permitted measurement of the performance of these devices directly. Rather, it has been necessary to infer performance from less direct terminal and probe measurements. The purpose of this paper is to describe efforts at direct performance measurement of a contemporary MPD thruster, and the results thereof.

Benchmark Thruster

One of the improved MPD configurations, termed the benchmark thruster, is shown schematically in Fig. 1. Although far from fully optimized, it does embody many of the features found to aid in raising the onset condition.

Presented as Paper 81-0684 at the AIAA/JSASS/DGLR 15th International Electric Propulsion Conference, Las Vegas, Nev., April 21-23, 1981; submitted March 22, 1982; revision received Sept. 13, 1982.

*Research Engineer, Dept. of Mechanical and Aerospace Engineering; presently Director, Experimental Research, GT-Devices, Inc., Alexandria, Va. Member AIAA.

†Research Engineer, Dept. of Mechanical and Aerospace Engineering; presently Staff Systems Scientist, RCA Astro-Electronics, Princecton, N.J. Member AIAA.

‡Dean, School of Engineering and Applied Science. Fellow AIAA.

Specifically, the thruster has a 10 cm long by 2 cm diam thoriated tungsten cathode, extending 4 cm past the anode plane. The anode is an annular aluminum disk of 20 cm o.d., with a 10 cm diam orifice. The rear insulator is boron nitrode and the side insulator a Pyrex tube of 12.5 cm i.d. The exterior of the thruster is insulated with a nylon sleeve.

The propellant injection system uses a modified commercial solenoid valve to provide a short pulse of propellant to a choked multiple orifice. This valve is driven by a 5000-μF capacitor charged to 150 V, triggered by an SCR at the start of the experiment. The multiple orifice splits the flow into two portions, one injected at the base of the cathode, and the remainder through a ring of 12 holes in the backplate, equally spaced at a radius of 3.8 cm. Two propellant divisions were used in these experiments, 54/46 and 0/100, through the annulus and through the 12 holes, respectively.

The time-profile of driving pressure at the choked orifice, as measured by a high-speed piezoelectric pressure transducer, is shown in Fig. 2. The figure shows that the mass pulse from this injection arrangement is more than ten times longer than the 1-ms thrust pulse. No attempt has been made for these single-shot experiments to minimize the total mass injected per pulse; clearly, that aspect will require further technological development. The values of specific impulse and efficiency quoted later are computed using only that fraction of the mass that is injected during the thrust pulse. In other words, the data are used to construct a quasisteady performance index which presumes that mass flow can ultimately be tailored to the arc current waveform.

Mass flow continuity during the 1-ms-long thrust pulse has been inferred from a variety of diagnostic data obtained previously. The most important of these are piezoelectric pressure measurements of both the arc chamber pressure and the impact pressure in the plasma exhaust flow.[2,8] Measured pressure at both locations reaches a steady value within about 200 μs of discharge initiation and maintains that value throughout the thrust pulse. Furthermore, integration of the radial profile of impact pressure over the exhaust plume yields a value for thrust within a few percent of that obtained from summing the electromagnetic and electrothermal components calculated from Eqs. (1) and (2). The possibility that the propellant flow is reduced by the chamber pressure during the discharge is inconsistent with the relative values of the measured chamber pressure (about 0.2 atm) and valve driving pressure (typically 4 atm), and with spectroscopic data which show that below the onset condition the exhaust is substantially comprised of argon neutrals and ions, with only trace amounts of the impurities characteristic of propellant starvation.[5]

In the quasisteady mode employed in these experiments, the current to the thruster is delivered in a rectangular pulse, in response to which the thruster switches on rapidly and operates in a steady fashion for several hundred microseconds. The existence of quasisteady operation has been verified previously by detailed electric and magnetic probe mappings of the thrust chamber and exhaust flow, which show that steady plasmadynamic conditions prevail within 200-300 μs of current initiation.[9,10]

The current waveform is provided by a 40 mΩ pulse-forming network (PFN) capable of delivering a single 50 kA $\times$ 1 ms current pulse. The PFN is matched to the 10 mΩ thruster impedance with a series 30 mΩ stainless steel resistor to prevent circuit ringing. Switching is provided by an evacuated gap, triggered by air injection 10 ms after the propellant valve is actuated to allow a steady mass flow to be established prior to the current pulse. Typical pulse shapes of arc current and voltage are shown in Fig. 3.

The operating range of the benchmark thruster for the experiments reported herein varies from 1.5-9.0 g/s argon, with current ranging from 7-26 kA. Results are also reported for nitrogen at 4 g/s, at currents from 24-30 kA.

Experimental Procedure

The thruster assembly, weighing approximately 20 kg, is cantilevered on a vertical axis, "swinging gate" thrust stand, shown schematically in Fig. 4. The mass is supported by two flexural pivots mounted on the hinge line, permitting horizontal rotation of the thruster and support arm. The restoring torque resulting from the current connectors, insulators, propellant feed, and instrumentation leads at the thrust stand pivot axis gives the system a natural frequency of 0.5-1 Hz. This small torque must be taken into account when reducing the thrust data, as discussed below.

The thruster and thrust stand are mounted in a dielectric vacuum tank 4.9 m in length by 1.9 m in diameter (Fig. 5). Total tank volume, including baffles, is about 20 m^3. A nylon mesh net covers the intakes to the twin 1.3-m diffusion pumps. The pressure drop across this net permits the pumps

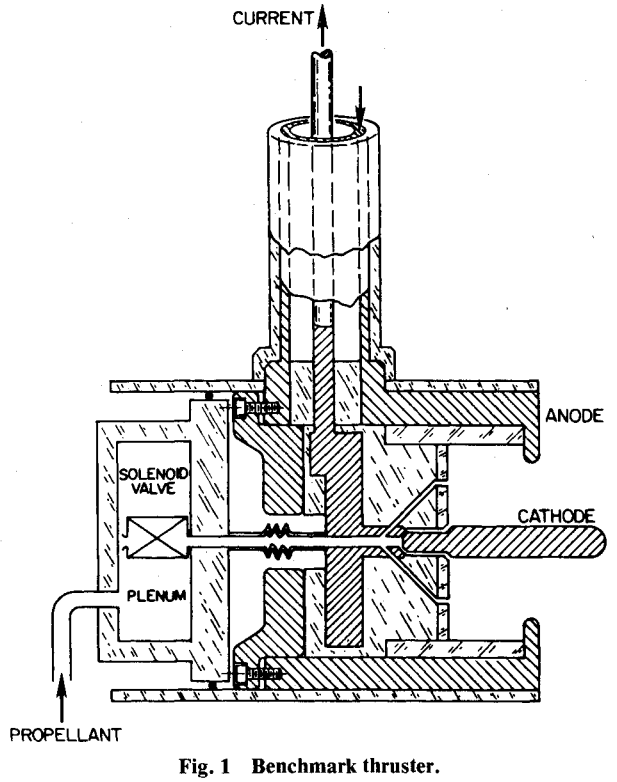

Fig. 1 Benchmark thruster.

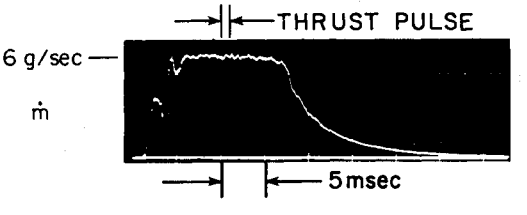

Fig. 2 Mass injection pulse.

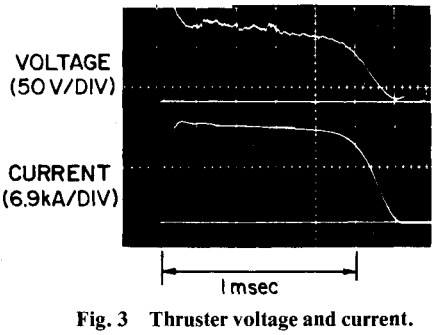

Fig. 3 Thruster voltage and current.

to recover more rapidly from a mass pulse which would otherwise exceed their breakback pressure (3×10^{-4} Torr). The recovery time of the vacuum system to $\sim10^{-5}$ Torr after the pulsed injection of 15 mg of argon is about 1 s, which will permit future repetitive thruster operation at a 1 Hz rate. For the experiments reported here, only single-shot operation every few minutes was employed.

The basic instrumentation provides measurement of four quantities: mass flow rate, current, voltage, and thruster position. The quasisteady mass flow is calibrated prior to the experiment by setting the pressure at the choked orifice equal to the constant value achieved during the mass flow pulse in Fig. 2, holding the propellant solenoid valve open for several minutes, and measuring the pressure rise in the evacuated vacuum tank with the pumps shut off. The data from this experiment are fit to a linear regression for a range of propellant supply pressures, and give a 2σ error (95% confidence) of 1% for the propellant flow rate.

Although the propellant pulse necessarily raises the initial tank pressure by the time of arc initiation, the two-way transit time for the injected argon to reach the far end wall of the tank and return is over twice the arc delay time, so that the ambient pressure in the vicinity of the thruster may be expected to remain below 10^{-4} Torr throughout the shot. Thrust errors due to propellant recirculation effects observed by others on steady-state thrusters[11] are therefore not a factor here.

Current is fed across the thrust stand hinge axis through flexible connectors of twisted braid which have negligible effect on the thrust impulse measurement, as verified by shorting the thruster electrodes and firing the bank. The current is measured by enclosing one of the external leads with a 500 turn Rogowski coil, which is integrated with an operational amplifier.

The arc voltage is measured outside the tank with a Tektronix 1000:1 high-voltage probe. The $L\dot{J}$ voltage drop between the measuring point and the thruster electrodes is negligible during the quasisteady period. An ohmic resistance of 1.07 mΩ between the voltage measuring point and the thruster was determined by shorting the electrodes and measuring the resulting resistive drop. The measured voltage was reduced by this resistive drop, typically 10-15 V, to give the thruster terminal voltage.

The thruster position throughout the stand recoil is measured with an 8 V/mm Bently-Nevada rf position transducer, chosen for its linear response to thruster motion. The transducer is fixed directly below the thruster axis, 0.61 m from the hinge axis, and measures the displacement of a 4140 alloy steel target mounted on the thruster (Fig. 6). Calibration is performed statically with a micrometer and digital voltmeter, and is found to be linear to within 1% over the range of 1.5 mm of motion permitted by the probe mount.

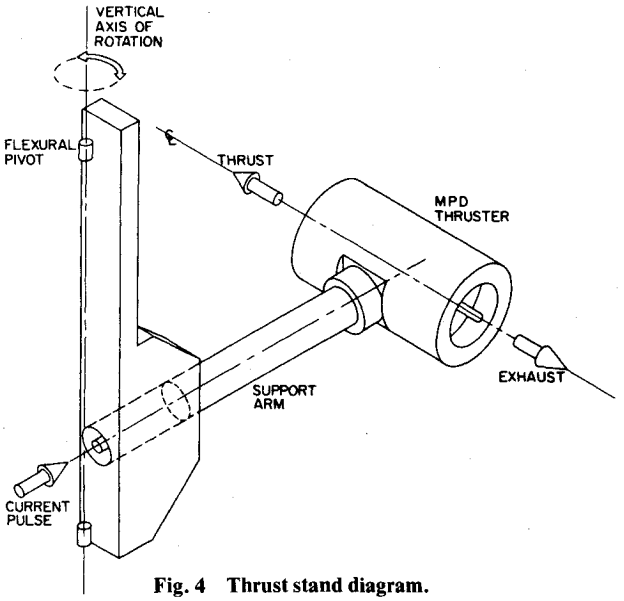

Fig. 4 Thrust stand diagram.

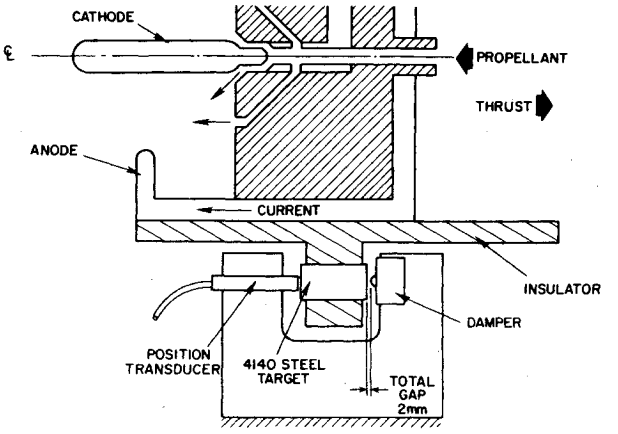

Fig. 6 Thrust stand instrumentation.

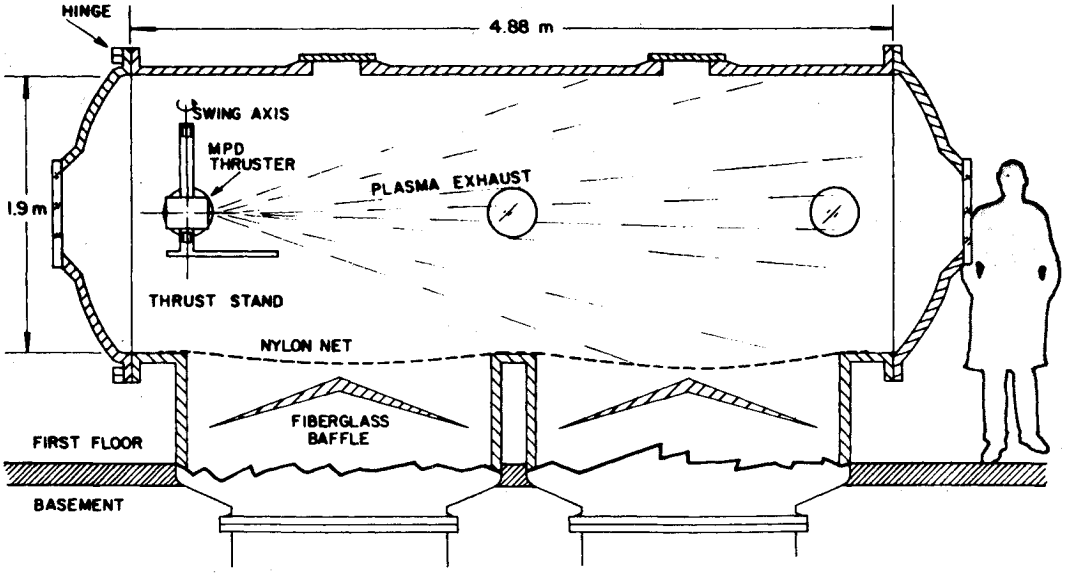

Fig. 5 Thrust stand installation in fiberglass tank.

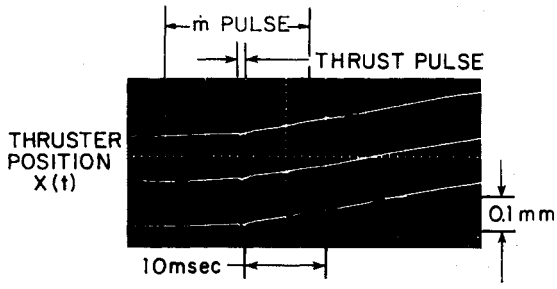

Fig. 7 Thrust stand response.

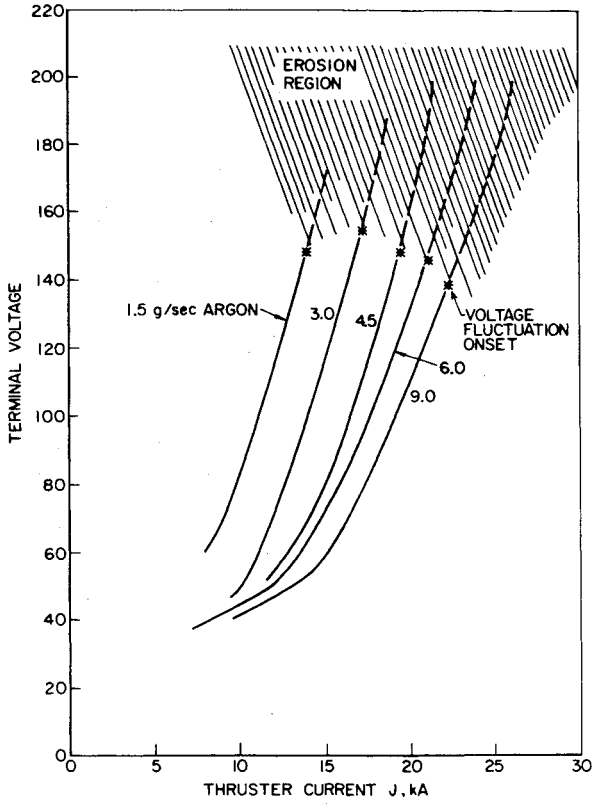

Fig. 8 Benchmark thruster voltage-current characteristics; 54/46 flow division.

A typical output signal from the position transducer is shown in Fig. 7, which displays three consecutive firings of the thruster. From its initial rest position, the thruster is first observed to move slightly after about 5 ms, in response to the start of the cold propellant pulse. The current pulse occurs at about 15 ms, after which the thruster achieves a much larger velocity increment. The net velocity change produced by the thrust pulse is obtained by subtracting the velocity increment due to the cold propellant injection from the total velocity change, as discussed below.

Because the thruster and thrust stand constitute a rotational system, the thrust changes the angular velocity, and hence the thruster position, in accordance with the relation

$$T = \frac{I}{R}\dot{\omega} = \frac{I}{R^2}\ddot{x} \tag{4}$$

The thrust measurement consists of measuring the impulse bit, given by

$$\int T\mathrm{d}t = \frac{I}{R^2}\Delta\dot{x} \tag{5}$$

where $\Delta\dot{x}$ is the change in thruster velocity during the thrust pulse. As mentioned, the impulse bit $\int T_c\mathrm{d}t$ due to the injection of cold propellant must be measured and subtracted from the total "hot" impulse bit $\int T_h\mathrm{d}t$ measured by firing the thruster.

The net impulse bit is thus given by

$$\int T\mathrm{d}t = \frac{I}{R^2}\left(\Delta\dot{x}_h - \Delta\dot{x}_c\right) \tag{6}$$

The empirical procedure consists of first measuring the "cold" impulse bit over a range of mass flows. The data are found to be linear with mass flow, consistent with a constant value of cold propellant exhaust velocity. From the measured argon mass flow pulse, this exhaust velocity is calculated to be 400 m/s, which is consistent with a supersonic expansion from a 300 K plenum. The "hot" impulse bit is then measured at each mass flow rate for a range of thruster currents. A typical data point consists of the mean of six or more shots. Since the thruster is initially at rest, only the final velocity need be measured, and the impulse bit may then be computed by Eq. (6).

In addition to the correction for cold flow thrust, the data are also corrected for the small residual torsion of the thrust stand, which tends to reduce the thruster drift velocity. This reduction is given by the ratio $(\sin\omega' t')/\omega' t'$, where ω' is the thrust stand natural angular frequency and t' is the time over which the thruster drift velocity is measured. This correction is typically 1-2%.

Results and Discussion

Voltage-Current Characteristics

The voltage-current characteristic for the benchmark thruster with argon is shown in Fig. 8 for a range of mass flows. The voltage increases strongly with current and decreases with mass flow, up to the voltage fluctuation onset and erosion regions. The onset condition occurs at about 150 V for argon, nearly independent of mass flow rate. The onset current ranges from 14-22.5 kA as mass flow increases from 1.5-9.0 g/s.

The effects on the voltage-current characteristic of changing the propellant type and flow division are shown in Fig. 9, which compares the characteristics for a 0/100 flow division for 6 g/s argon and 4 g/s nitrogen with the previous 54/46 flow division, 6 g/s argon case shown in Fig. 8. The onset voltage for argon is still approximately 150 V, but since the voltage is lower at all currents, the onset current is increased from 21kA to 27kA. This implies increased thruster efficiency when no propellant is injected at the base of the cathode. For nitrogen at 4 g/s, the onset occurs at 275 V and 30 kA. The thruster impedance for nitrogen remains at 8-9 mΩ over the current range of 24-30 kA for which data were recorded.

Thrust

Because the primary thrust data are in the form of impulse bits, a thrust-time profile must be assumed in order to deduce the instantaneous performance values during a given pulse. In our case, where the current waveform is nearly flat and the thrust is dominated by the electromagnetic term, less than 1% error is introduced by assuming that thrust scales as the square of the current throughout the pulse. The proportionality constant b is obtained from the integral relation

$$\int T\mathrm{d}t = b\int J^2\mathrm{d}t \tag{7}$$

using the measured impulse bit and the known current waveform.

The resulting typical values of thrust for argon with a 54/46 flow division are shown in Fig. 10. Also shown in the figure is the electromagnetic thrust for the 6 g/s case as calculated from Eq. (1). To obtain accurate values of current attachment radii for use in this equation, the current distributions at anode and cathode were mapped by detailed magnetic probing of the discharge.[12] For the benchmark thruster, the measured

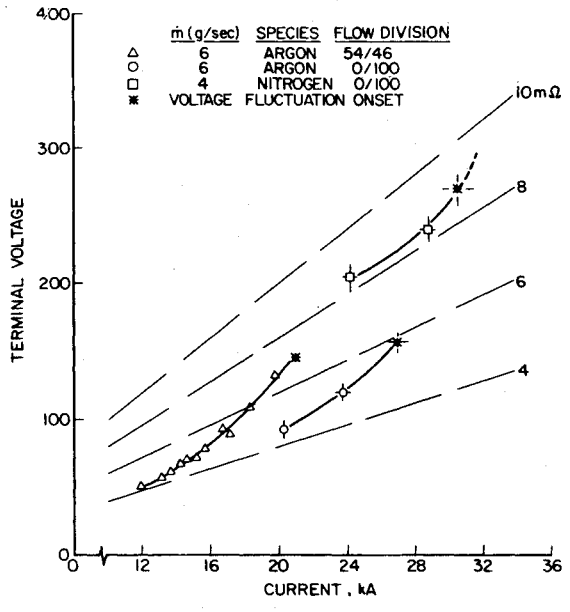

Fig. 9 Voltage-current characteristics; benchmark thruster.

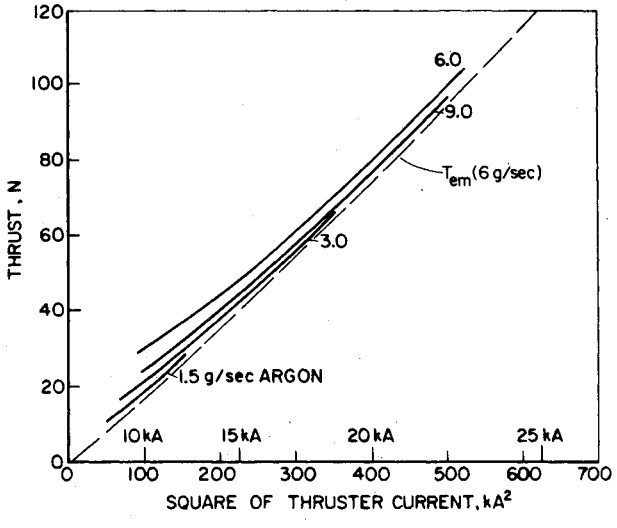

Fig. 10 Quasisteady thrust; benchmark thruster.

distributions indicated that the constant C is negligibly small, and the effective ratio of current attachment radii is given by

$$r_a/r_c = 5.63 + 0.011\, J^2/\dot{m} \tag{8}$$

where the units of J and $\dot{m}$ are kA and g/s, respectively. According to this expression, the current attachment occurs near the anode lip ($r_a/r_c = 5.33$) at low currents, and moves slightly outward with increasing current to a maximum value of $r_a/r_c = 6.7$. The overall effect on the electromagnetic thrust component of these variations in r_a/r_c is about 10% over the range of currents tested.

Figure 10 shows that at low current the measured thrust is significantly greater than the calculated electromagnetic thrust, due to a sizable electrothermal component. As the current increases, the electromagnetic component becomes more dominant. The approach of the measured thrust to the calculated electromagnetic value occurs at lower currents for lower mass flows. Note that since the measured thrust is greater than the calculated electromagnetic component at all currents and mass flows, early estimates of MPD performance, based solely on that component, were correspondingly conservative.

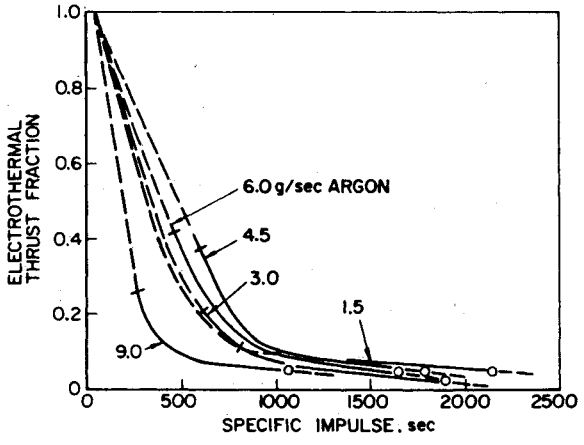

Fig. 11 Electrothermal thrust fraction.

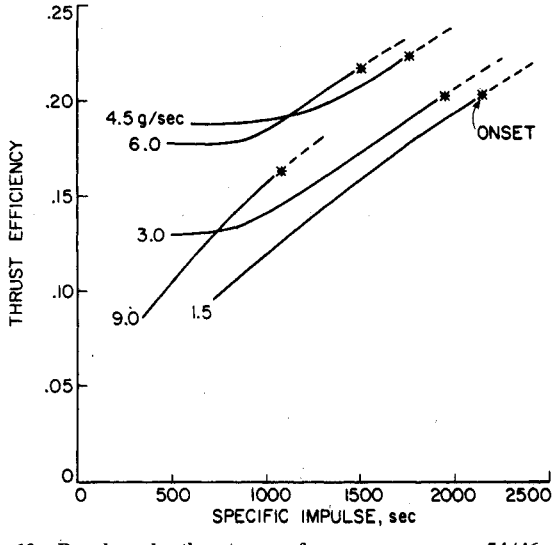

Fig. 12 Benchmark thruster performance; argon, 54/46 flow division.

The electrothermal component of thrust is shown in Fig. 11 as a function of specific impulse, for various argon mass flows. For specific impulses below 1000 s, the electrothermal fraction is quite consequential; above that value, it is less than 10% of the total thrust, for all mass flows tested.

Quasisteady Performance

The current and voltage measured during the quasisteady portion of the discharge may be combined with the thrust measurements to provide quasisteady values of specific impulse and thrust efficiency, using the relations

$$I_{sp} = \frac{bJ^2}{\dot{m}g} \tag{9}$$

$$\eta = \frac{T^2}{2\dot{m}VJ} = \frac{b^2J^3}{2\dot{m}V} \tag{10}$$

The resulting performance map of the benchmark thruster is shown in Fig. 12 for argon mass flows from 1.5-9.0 g/s and a 54/46 flow division. Figure 13 compares this performance with 0/100 flow division data for argon (6 g/s) and nitrogen (4 g/s). The curves in both figures are drawn through data points which represent the mean of six shots, and the typical error bars indicate one standard deviation of the data. The systematic error associated with each value of specific impulse, as derived from the calibration of the thrust stand and mass flow rate, is ±3% of the values shown. Similarly, the systematic error for each value of efficiency is ±10%.

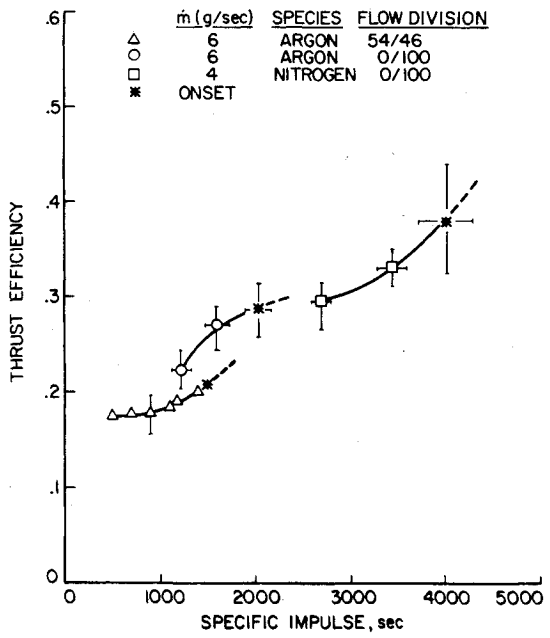

Fig. 13 Benchmark thruster performance.

Several features of these data are noteworthy:

1) For a given mass flow, the efficiency increases monotonically with specific impulse, up to the limit imposed by thruster erosion at or above the onset point.

2) For a given thruster configuration, propellant species, and distribution, the best operating point is a function of the mass flow. For example, maximum efficiency with a 54/46 argon propellant division is achieved with a total mass flow of about 4.5 g/s. The thrust efficiency at this point is 22% and the specific impulse is 1750 s. The maximum specific impulse of 2150 s is obtained at a lower mass flow, about 1.5 g/s, for which the efficiency drops slightly to 20%.

3) The effect of electrothermal thrust is more pronounced at low specific impulse, tending to raise the efficiency and thereby reducing the penalty for operating off the peak efficiency point.

4) Injecting relatively more propellant near the anode displays the dual advantages of a higher efficiency for a given operating point, as characterized by J and $\dot{m}$ and therefore by I_{sp}, and the ability to operate at a higher specific impulse and efficiency before erosion is encountered. By this technique, an efficiency of 28.5% at 2000 s is attained for 6 g/s argon.

5) Nitrogen propellant displays consistently higher specific impulses and efficiencies, reaching 38% at 4000 s.

Summary

The anticipated interesting performance capability of the MPD thruster previously inferred by indirect measurements has been confirmed by direct measurement of impulse bits. The data show that at low specific impulses the electrothermal contribution is somewhat higher than expected, but in the more interesting high specific impulse range, it appears to contribute only a few percent to the total thrust, as previously predicted.[10] The thrust efficiency lies correspondingly above that predicted previously from detailed magnetic probing of the MPD discharge.

It should be stressed that the performance data displayed here apply only to this particular design, and should not be interpreted to represent the ultimate performance of this class of MPD thruster. The improved performance resulting from the small excursions in propellant species and distribution described here clearly establish the sensitivity of the performance to such parameters. It is fully expected that more extensive measurements of this and other improved geometries will display yet higher values of specific impulse and efficiency.

Acknowledgments

Much of the burden of the construction and calibration of the thrust stand facility, and of the conduct of the experiments, was borne by A.L. Casini and C.G. Carlson. This work has been supported by JPL Contract 955917.

References

[1] Jahn, R.G., *Physics of Electric Propulsion*, McGraw-Hill Book Co., New York, 1968.

[2] Cory, J.S. and Jahn, R.G., "Mass, Momentum and Energy Flow from an MPD Accelerator," Aerospace and Mechanical Sciences Rept. No. 999, Princeton University, Princeton, N.J., Sept. 1971.

[3] Rudolph, L.K., Jahn, R.G., Clark, K.E., and von Jaskowsky, W.F., "Onset Phenomena in Self-Field MPD Arcjets," AIAA Paper 78-653, April 1978.

[4] Rowe, R.A., von Jaskowsky, W.F., Clark, K.E., and Jahn, R.G., "Erosion Measurements on Quasi-Steady MPD Thrusters," *Journal of Spacecraft and Rockets*, Vol. 19, July-Aug. 1982, pp. 349-353.

[5] Rudolph, L.K. and Jahn, R.G., "The MPD Thruster Onset Current Limitation," Mechanical and Aerospace Engineering Rept. No. 1491, Princeton University, Princeton, N.J., Sept. 1980.

[6] King, D.Q., Smith, W.W., Jahn, R.G., and Clark, K.E., "Effect of Thrust Chamber Configuration on MPD Arcjet Performance," *Electric Propulsion and Its Applications to Space Missions*, Vol. 79, Progress in Astronautics and Aeronautics, 1981, pp. 504-517.

[7] Ho, D.D. and Jahn, R.G., "Erosion Studies in an MPD Thruster," Mechanical and Aerospace Engineering Rept. No. 1515, Princeton University, Princeton, N.J., May 1981.

[8] Clark, K.E., Jahn, R.G., and von Jaskowsky, W.F., "Measurements of Mass, Momentum and Energy Distributions in a Quasi-Steady MPD Discharge," AIAA Paper 72-497, April 1972.

[9] Clark, K.E. and Jahn, R.G., "Quasi-Steady Plasma Acceleration," *AIAA Journal*, Vol. 8, Feb. 1970, pp. 216-220.

[10] Rudolph, L.K., Jahn, R.G., Clark, K.E., and von Jaskowsky, W.F., "Performance Characteristics of Quasi-Steady MPD Discharges," AIAA Paper 76-1000, Nov. 1976.

[11] Sovie, R.J. and Connolly, D.J., "Effect of Background Pressure on Magnetoplasmadynamic Thruster Operation," *Journal of Spacecraft and Rockets*, Vol. 7, March 1970, p. 255.

[12] Kaplan, D.I., "Performance Characteristics of Geometrically Scaled MPD Thrusters," Mechanical and Aerospace Engineering Rept. No. 1492, Princeton University, Princeton, N.J., Feb. 1982.